International Journal of Aquatic Science
ISSN: 2008-8019
Vol 12, Issue 02, 2021

Investigations On Thermal Behavior Of Vmc Base Made Of Epoxy Granite

A. Aravindh[1], P.R.Thyla[2], M. Kalayarasan[3]

[1]PG Scholar, Department of Mechanical Engineering, PSG College of Technology.
[2]Professor, Department of Mechanical Engineering, PSG College of Technology.
[3]Assistant professor (Sr. Gr), Department of Mechanical Engineering, PSG College of Technology.

Email; prt.mech@psgtech.ac.in.[2]

Abstract: In a vertical machining centre (VMC) heat generation occurs due to the movement of the machine tool components. This heat generationand surrounding air temperature create temperature rise in the machine tool. Due tothe temperature rise, the tool centre point (TCP) displaces which leads to inaccuracy and loss of precision in machined components. VMC base is one of the major componentsof a machine tool contributing to TCP displacement. In VMC base, thermal deformation of the guideway is caused by heat generation of linear motion bearing, and thermal deformation of the feed drive system is caused by ball screw movement. Further, the ball bearing also contributes to TCP displacement. Epoxy granite is used as a replacement for conventional cast iron in VMC base due to its better dynamic characteristics. But the lower thermal conductivity of epoxy granite, makes the heat to concentrate in a localised region which creates structural deformation. The present work focuses on determination of heat generation due to the frictionof linear motion bearing and feed drive system, the corresponding temperature rise and deformation of the VMC base. A mathematical model based on transfer function is also developed to predict thermal errors.

Keywords: VMC base, TCP displacement, Transfer function, Epoxy granite.

1. INTRODUCTION

Machine tool errors can be classifiedas geometric and kinematic errors, thermal errors, errors induced due to cutting forceand tool wear errors.One of the major factors contributing to machine tool accuracy is thermal errors and thermal errors account for nearly 40%-70% of the total error (1). Two kinds of heat sources cause thermal errors in machine tools: the are, external heat sources and internal heat sources. The external heat sources are environmental temperature variations. The internal heat sources are heat generated in spindle, ball screw, guideways and driving motor (2). Thermal errors are caused by the heat generated in the moving componentsand environmental temperaturevariations (3). Feed drive system is responsible for positioning of machine tool components, cutting tool and work pieceand therefore their positioning accuracy and speed determines the productivity and quality of the machine tool. Recirculating rolling guide generates negligible heat under free load condition, but under machining conditions it generates considerable heat and thermal errors on the guideway of the base also should be considered.

Thermal errors can be reduced by modifying the machine tool structure (4), it can be reduced by controlling the machine tool temperature by the application of coolant (5), it can also be reduced by predicting and compensating thermal error by formulating mathematicalmodels (6). Mathematical model for compensating thermal errors should be installed in tool control for precise operation of machine tools. The input variables required to formulate a mathematical model can be found by design of experiments statistical tool (7)Environmental temperatureand loading of the ball screw affect the thermal deformation of the ball screw. Real time data such as current, velocity of the driving motor, displacement of axes can also be utilized to derive the thermal deformation model (8). Frictional heat generated by the linear motion bearing should be estimated to find the thermal deformation of the machine tool guideway (9).The thermal error of the machine tool is affected by the environmental temperature also (10).

Heat generated by the ball screw can be found by both the energy method and formula method, results of which are good enough as inputs for finite element analysis (FEA). The temperature rise of the system can be found by FEA (11). Thermal deformation of the ball screw is affected by its loading conditions, multiple linear regression is used as mathematical model to compensate the thermal deformation caused by the ball screw (12). A robust modelling method based on heat transfer theory can be used to model the ball screw system. The ball screw is divided into number of segments and the temperature rise at each segment is studied (13). Transfer function serves as better mathematical model in compensation systems compared to multiple linear regression, further it has been tested by machining a test workpiece (14). Machine tool spindle thermal error can be compensated by transfer function and linear regression. Transfer function compensated better compared to linear regression (15).

However few researches focused on the cast iron as the VMC base material, where the guideway deformation is negligible since cast ironhas good thermal conductivity and low coefficient of thermal expansion. Epoxy granite, which is a stone-based composite, is increasingly beingused as machine tool structural material. It has good static and dynamic characteristics, but its low thermal conductivity and high thermal expansion coefficient cause more structural deformation compared to cast iron. This paper considers epoxy granite as material for the base of VMC and quantify the thermal deformation of the guideway and feed drive system. Transfer function is used as the mathematical model to predict the thermal error of the VMC base.

DETERMINATION OF THERMAL LOADS AT THE GUIDEWAY OF VMC BASE

Machine tool and bearing model

VMC BT-40 1060V is a powerful and compact foot print machine with front disposable system suitable for a variety of applications. It is loaded with 24 tool ATC and high-speed spindle. The spindle motor used is 7.5kW FANUC. The column and the base of the machine tool are made up of cast iron. It is proposed to change the machine tool base material to epoxy granite, since it is rapidly replacing cast iron due to better dynamic and static characteristics.The propertiesof thematerial are:density(ρ)=$2300 kg/m^3$, Thermal expansion(α)=17 μm/mK,Isotropic thermal conductivity(K)=0.410W/m℃, Specific heat(C)= 832 J/kg℃,Young's modulus(Y)=30 GPa, Poisson's ratio(μ)=0.25

Table 1. Machine tool specifications

Description	**Magnitude**
Table size(mm)	1200X600
Maximum load on the table (N)	6380
Z-axis assembly Stroke(mm) Spindle nose to table(mm)	 400 150-550
X-axis assembly Stroke(mm)	 600
Y-axis assembly Stroke(mm)	 400
Spindle assembly Spindle nose taper Maximum speed (RPM)	 7/24 No.40 6000

The linear bearing model used is HSR30 LRwhere HSR30 denotes the dimensions of the slider and LR denotes the length of the rail. The travelling distance of the linear motion bearing is limited by the length of the rail.

Table 2. Specifications of linear motion bearing

Description	**Magnitude**
Length of the bearing(mm)	93
Static load rating(kN)	37.3
Basic load rating(kN)	62.5
Height of the LM block(mm)	45
Width of the LM block(mm)	60
Length of the LM block(mm)	120
Rail length (mm)	2520
Rail width(mm)	28
Rail height(mm)	26

Calculation of dynamic load in guideways.

Loads acting on linear bearings and guides can be vertical loads, horizontal loads or pitch roll or yaw moment loads, or any combination of these loads. Loads may vary in their magnitude and direction. In bearings, equivalent dynamic load is calculated to account for all loading conditions.The equivalent dynamic load calculated is a hypothetical load, of constant magnitude and direction, which would have the same influence on the bearing life as the actual load.The dynamic load capacity, C, is based on empirical testing in which a load that is constant in magnitude and normal to the load-bearing surfaces allows the bearing to achieve a defined travel distance (linear guide) or number of revolutions (ball screw) without fatigue. A co-ordinate system must be assigned to find the centroid of the model as shown in Fig.1. The centre of gravity (CG) of linear motion bearing from the centroid of the model is taken as the

point of application of force as shown in Fig.2. The load due to weight, process force, and acceleration force act at the centre of gravity of the linear motion bearing.

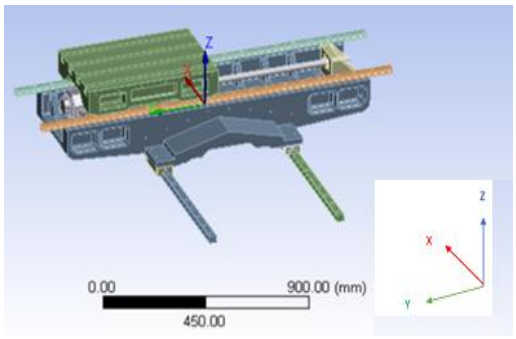

Fig. 1.New coordinate system

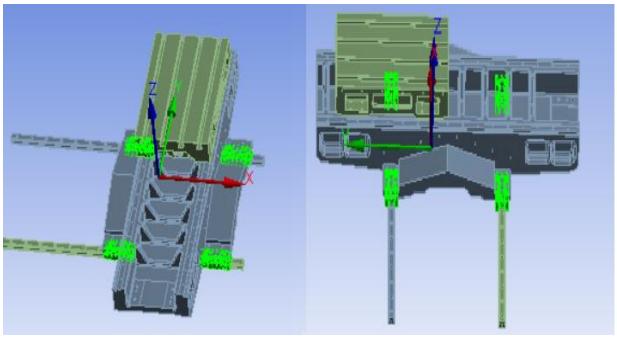

Fig.2.Location of Centre of gravity of slider

The total weight is obtained by summation of mass of the machine table (638 kg) and the capacity of the machine table (300 kg). The x,y and z locations of the center of gravity of sliders are shown in Table 3.

Table 3. Locations of enter of gravity of sliders

Parameter	**Slider-1**	**Slider-2**	**Slider-3**	**Slider- 4**
X-coordinate of center of gravity(mm)	312	-211	312	-211
Y-coordinate of center of gravity(mm)	286	286	-303	-303
Z-coordinate of center of gravity(mm)	-122	-122	-122	-122

The load acting on the bearings are lift-off loads, side-loads,and downward acting loads.These loads are transmitted through two rows of the rolling elements. The lift off loads and downward acting loads act in the positive and negative directions of Z axis. The side loads act in the lateral direction along Y axis.The inertial forces during acceleration and deceleration act along X- axis. The load case calculation is divided into three phases. In phase-1 the weight force and acceleration forces act. In phase-2 the weight force and process forces act. In phase-3 weight force and deceleration force act.

Table 4.Assigning load case and phases for each force in bearing

Load case j	Description	Effective force $\mathbf{F_{w,j}}$	Phase n
1	Weight	$\mathbf{F_{wz,1} = F_g = -9202N}$	1;2;3
2	Inertial force during acceleration $\mathbf{a_1 = 2m/s^2}$	$\mathbf{F_{wx,2} = F_{a1} = -1876N}$	1
3	Cutting force during machining	$\mathbf{F_{wy,3} = F_p = -4500N}$	2
4	Inertia force during deceleration $\mathbf{a_3 = -2m/s^2}$	$\mathbf{F_{wx,4} = F_{a3} = 1876N}$	3

The load case and its force application point on each slider is shown in Table 5.

Load case j	Force application point $x_{w,j}, y_{w,j}, z_{w,j}$				Phase n
	Slider1	Slider2	Slider3	Slider4	
1	$x_{w,1} = x_s = 312mm$ $y_{w,1} = y_s = 286mm$ $z_{w,1} = z_s = -122mm$	$x_{w,1} = x_s - 212mm$ $y_{w,1} = y_s = 286mm$ $z_{w,1} = z_s = -122mm$	$x_{w,1} = x_s = 312mm$ $y_{w,1} = y_s = -304mm$ $z_{w,1} = z_s = -122mm$	$x_{w,1} = x_s = -212mm$ $y_{w,1} = y_s = -304mm$ $z_{w,1} = z_s = -122mm$	1;2;3
2	$x_{w,2} = x_s = 312mm$ $y_{w,2} = y_s = 286mm$ $z_{w,2} = z_s = -122mm$	$x_{w,2} = x_s = -212mm$ $y_{w,2} = y_s = 286mm$ $z_{w,2} = z_s = -122mm$	$x_{w,2} = x_s = 312mm$ $y_{w,2} = y_s - 304mm$ $z_{w,2} = z_s = -122mm$	$x_{w,2} = x_s = -212mm$ $y_{w,2} = y_s = -304mm$ $z_{w,2} = z_s = -122mm$	1
3	$x_{w,3} = x_s = 312mm$ $y_{w,3} = y_s = 286mm$ $z_{w,3} = z_s = -122mm$	$x_{w,3} = x_s = -212mm$ $y_{w,3} = y_s = 286mm$ $z_{w,3} = z_s = -122mm$	$x_{w,3} = x_s = 312mm$ $y_{w,3} = y_s - 304mm$ $z_{w,3} = z_s = -122mm$	$x_{w,3} = x_s = -212mm$ $y_{w,3} = y_s - 304mm$ $z_{w,3} = z_s = -122mm$	2
4	$x_{w,4} = x_s = -212mm$ $y_{w,4} = y_s = 286mm$ $z_{w,4} = z_s = -122mm$	$x_{w,4} = x_s = -212mm$ $y_{w,4} = y_s = 286mm$ $z_{w,4} = z_s = -122mm$	$x_{w,4} = x_s = 312mm$ $y_{w,4} = y_s = -304mm$ $z_{w,4} = z_s = -122mm$	$x_{w,4} = x_s = -212mm$ $y_{w,4} = y_s = -304mm$ $z_{w,4} = z_s = -122mm$	3

Table 5. Load case application point on each slider

$$\mathbf{F_{z1\,3}} = \frac{F_{wz,1}}{4} + \frac{-(F_{wz,1}.y_{w,1})}{2.L_S} + \frac{(F_{wz,1}.x_{w,1})-(F_{wx,2}.z_{w,2})}{2.L_S} \quad (1)$$

$\mathbf{F_{z1\,3}}$-Force in z direction in phase 1 in slider 3

Similarly, forces along z direction for sliders 1,2, and 4are also calculated for phase-1.

For $\mathbf{x_{w,i}, y_{w,i}, z_{w,i}}$ values are given in Table 5

$$F_{y,1\,3} = \frac{-(F_{wx,2}.y_{w,2})}{2.L_w} = 544N \quad (2)$$

$F_{y,1\,3}$ - Force in y direction in phase 1 in slider 3

Using the above procedure, forces along y direction for sliders 1,2, and 4 are also calculated for phase-1.

For $x_{w,i}, y_{w,i}, z_{w,i}$ values refer Table5

$$F_{z2\,3} = \frac{F_{wz,1}}{4} + \frac{(F_{wy,3}.z_{w,3}) - (F_{wz,1}.y_{w,1})}{2.L_S} + \frac{F_{wz,1}.x_{w,1}}{2.L_w} \quad (3)$$

$F_{z2\,3}$- Force in z direction in phase 2 in slider 3.

Forces along z direction for sliders 1,2, and 4 are also calculated for phase-2.

For $x_{w,i}, y_{w,i}, z_{w,i}$ values refer Table 5

$$F_{y2\,3} = \frac{F_{wy,3}}{4} + \frac{F_{wy,3}.x_{w,3}}{2.L_w} = -1984N \quad (4)$$

$F_{y2\,3}$ - Force in y direction in phase 2 in slider 3.

Forces along y direction for sliders 1,2, and 4 are also calculated for phase-2.

For $x_{w,i}, y_{w,i}, z_{w,i}$ values refer Table5.

$$\mathbf{F_{z3\,3}} = \frac{\mathbf{F_{wz,1}}}{\mathbf{4}} + \frac{-(\mathbf{F_{wz,1}}.\mathbf{y_{w,1}})}{\mathbf{2.L_S}} + \frac{(\mathbf{F_{wz,1}}.\mathbf{x_{w,1}}) - (\mathbf{F_{wx,4}}.\mathbf{z_{w,4}})}{\mathbf{2.L_W}} \quad (5)$$

$\mathbf{F_{z3\,3}}$- Force in z direction in phase 3 in slider 3

For $\mathbf{x_{w,i}, y_{w,i}, z_{w,i}}$ values refer Table5

$$F_{y3\,3} = \frac{-(F_{wx,4}.y_{w,4})}{2.L_W} = 544N \quad (6)$$

$F_{y3\,3}$ - Force in y direction in phase 3 in slider 3

For $x_{w,i}, y_{w,i}, z_{w,i}$ values refer Table5.

For external load acting on a bearing for different phases in two directions, a combined load must be obtained which is the absolute value of forces F_z and F_y (10).

Phase :1

$F_{comb\,1\,3} = |F_{z1\,3}| + |F_{y,1\,3}| = 2089N$

Phase :2

$F_{comb\,2\,3} = 11300N$

Phase :3

$F_{comb\,3\,3} = 7733N$

$F_{comb\,1\,3}$ = Combined equivalent load on the bearing in phase 1 in slider 3

$F_{comb\,2\,3}$ = Combined equivalent load on the bearing in phase 2 in slider 3

$F_{comb\,3\,3}$ = Combined equivalent load on the bearing in phase 3 in slider 3

Effective equivalent load is calculated by considering the preload. Preload is actually applied to reduce the deflection characteristics of the system as a whole, but if more preload is applied, then the resistance to movement becomes greater.

$$F_{eff\,1\,3} = \left(\frac{F_{comb\,1\,3}}{2.8 \times F_{pr}} + 1\right)^{1.5}.F_{pr} = 9965N \quad (7)$$

F_{pr} - preload which is 8% of dynamic load capacity(62500N**)**from (11).

F_{pr} = 5000N

$F_{eff\,2\,3}$= 12147N

$F_{eff\,3\,3}$= 9671N

$F_{eff\,1\,3}$ = Effective equivalent load on bearing in phase 1 in slider 3.

$F_{eff\,23}$ = Effective equivalent load on bearing in phase 2 in slider 3

$F_{eff\,33}$= Effective equivalent load on bearing in phase 3 in slider 3

Similarly, effective equivalent load for remaining sliders can also be found out. Equivalent dynamic load for a linear motion bearing depends upon discrete travel step during each phase. Equivalent dynamic load is determined when loads alternate frequently during operation.

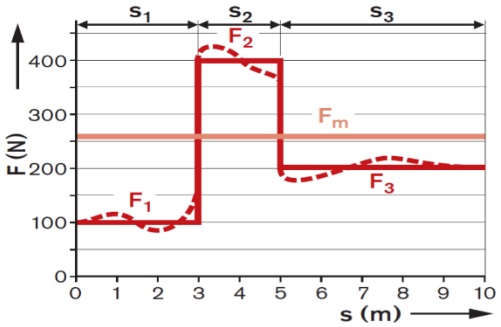

Fig.3Discrete travel steps for the three phases

Fig.3 represents the load variations and the corresponding distance travelled during three phases. The three phases constitute a cycle. Cycles are distance dependent for linear motion (11), so the equivalent dynamic load is calculated by multiplying individual effective load by distance covered expressed in percentage. --- denotesactual force profile of the linear motion bearingduring the three phases, which is approximated and the average force (F_m) over the entire cycle is calculated which is the equivalent dynamic load.The discrete travel step ($\mathbf{q_{si}}$) can be obtained by dividing the distance of individual cycle distance (s_1, s_2, s_3) by the total cycle distance(s). The discrete travel step for phase-1 is 12.5%, for phase-2 –75%, for phase-3-12.5%.

$$\mathbf{F_{mi}} = \sqrt[3]{(\mathbf{F_{eff\ 1\ i}})^3.\frac{\mathbf{q_{s1}}}{\mathbf{100\%}} + (\mathbf{F_{eff\ 2\ i}})^3.\frac{\mathbf{q_{s2}}}{\mathbf{100\%}} + (\mathbf{F_{eff\ 3\ i}})^3.\frac{\mathbf{q_{s3}}}{\mathbf{100\%}}}$$

The equivalent dynamic load acting on the four sliders are as follows:

$$F_{m1} = 10473\ N$$
$$F_{m2} = 7827N$$
$$F_{m3} = 11649N$$
$$F_{m4} = 7622N$$

Calculation of heat flow rate due to frictional force

The equivalent dynamic load is used to calculate the frictional force, using which heat generation can be estimated.The frictional force equation adopted by Sung-Hyun Jang1 et. al, (10), who have used the same bearing, viz., HSR30LR. Experiments have been carried out to measure the frictional force corresponding to velocity of linear motion bearing and its preload class (10).From the experimental values using Box–Behnken design (statistical technique) linear or quadratic expression is estimated (10)

Friction force(F_f) = 6.395 + 21.55V + 5.51871× 10^{-4}F- 4.5675p_b+ 5V^2+ 4.30955 × $10^{-8}F^2$ + 5.6225p_b^2 + 4.9V p_b+5.27211 × 10^{-5}F p_b(9)

V- velocity of slider in m/s = 0.45m/s

F- equivalent dynamic load in N = 11649N

p_b- Preload class=2µm (heavy)

Frictional force generated due to the movement of linear motion bearing on the rail (F_f) =27N.

Heat generation due to friction force is given by

(Q)= $\eta \times F_f \times$V(10)

η= 1 implies that frictional force is fully converted to heat. Heat generation rate is(Q)=12.15W and the heat flux(q) which can be found out with dimensions of the rail, is

Heat flux(q)= 1.85×10^{-4} W/mm^2.

Thus, to account for all the forces acting on the bearing, calculation of equivalent dynamic load is necessary. The frictional force depends upon the equivalent dynamic load, velocity and bearing preload class. Heat generation rate depends upon the velocity, and friction force of the bearing. The heat fluxdetermined is given as an input to the finite element model of VMC base.

THERMOMECHANICAL ANALYSES OF THE GUIDEWAY OF VMC BASE

Temperature change in guideway due to ambient and heat flow

Heat flux is defined as the amount of heat transferred per unit area per unit time from or to a surface. The heat flux obtained as a result of heat generation in linear motion bearing is applied at the guideway of the base as shown in Fig.4The ambient temperature is the temperature of the air in a particular region above the ground. The temperature of the surrounding air is not constant, it changes depending upon seasons, and time of the day. There is a convection heat transfer between the system and surrounding air, with a film coefficient as shown in Fig.3. The heat transfer between the surrounding and the machine base is considered as free convection. The heat flux and convection cause the temperature of the system to change.

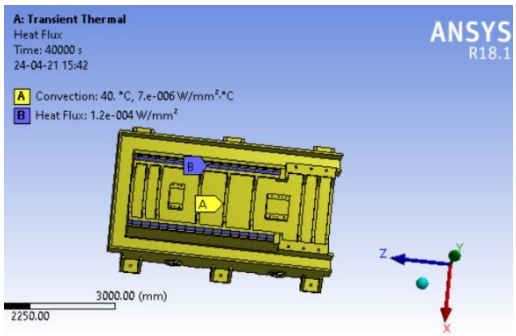

Fig.4. Boundary conditions of VMC base

It is observed from Fig.5 that the temperature varies up to a time period of 8 hours, or the system takes 8 hours to reach steady state. Therefore, the time constant of the system is large. Maximum temperature of 52^0C occurs at the guideway, while a temperature range of 40 to 45^0C occurs at the edges and vertices of the guideway, other regions of the VMC base have temperatures slightly higher than ambient temperature as shown in Fig.5.

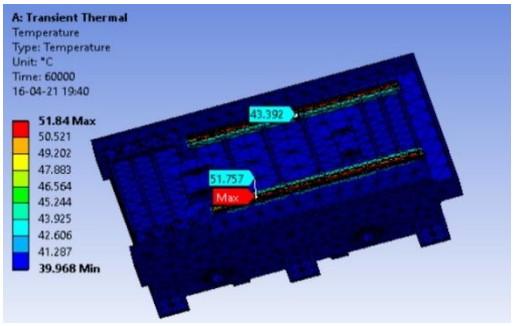

Fig.5.Temperature distributionin guideway of VMC base

International Journal of Aquatic Science
ISSN: 2008-8019
Vol 12, Issue 02, 2021

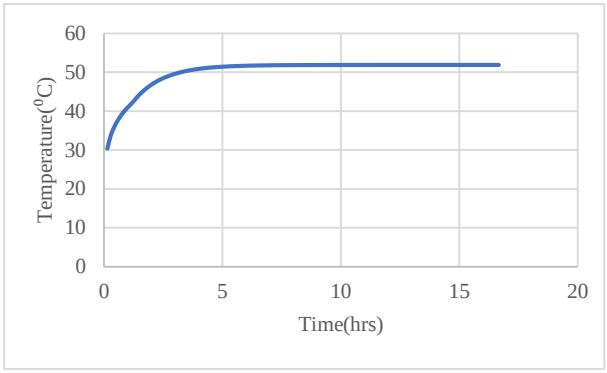

Fig.6.Transient variation of temperature ofthe guideway of VMC base

There is a deformation in the guideway of the VMC base due to the temperature rise caused by the heat generated in the linear motion bearing and convection caused by surrounding air. This deformation results in the displacement of the table which leads to the offset of TCP of the machine tool.

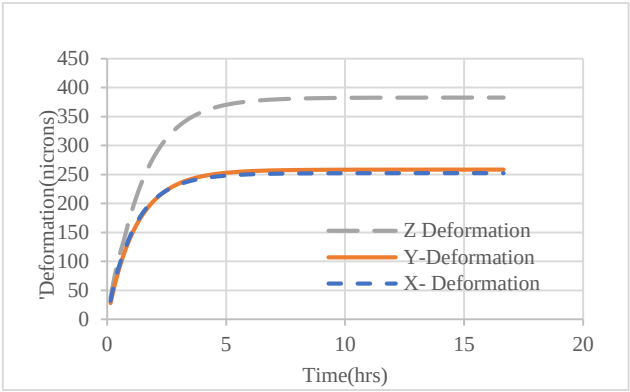

Fig.7.Transient variation of deformation of the guideway of VMC base

The deformation is not constant, it varies with respect to time. Maximum deformation occurs at the time where temperature is maximum and thereafter the deformation remains constant.The deformation in the X, Y and Z directions is caused due to the temperature change of the guideway. Depending upon the symmetricity and asymmetricity of the base, the deformation along positive and negative co-ordinates may vary. Fig.7 shows the deformation of the guideway along X, Y and Z directions.

THERMAL ANALYSIS OF FEED DRIVE SYSTEM

Components of feed drive system

The feed drive system consists of ball screw shaft, ball screw and nut assembly, support bearings, and drive motor. The ball screw is also known as recirculating ball screw or ball bearing screw. Preloading is done to ensure that ball is in contact with screw and nut. The support bearings mounted on the ball screw shaft support the axial load induced by the drive motor and the ball screw nut. The ball screw shaft and nut model used is THK 2004-10 model. Back-to-back front bearing 7905 A5 DB is used for front bearing, since axial loads along two directions are to be supported. At the rear end, axial load in one direction is to be supported, so single bearing of type 7905 A5 is used.

Heat generation due to friction between the ball screw shaft and ball nut.

Two types of friction exist between the ball screw shaft and the ball nut. Due to the applied preload in ball nut system an increase in friction occurs, as a result heat is generated. Preloading is done to maintain the accuracy and rigidity. Viscous friction from ball screw rotation also generates heat. The total frictional torque is given by the sum of the load friction torque and preload torque. Axial load is required to drive the feed drive system, the axial load is not constant for a cycle, it varies during acceleration, deceleration and uniform motion. The average axial load required to drive the feed drive system has to be found. The travel distance during acceleration ($l_{1,4}$), deceleration ($l_{2,5}$) and uniform motion ($l_{3,6}$) has to be calculated to find the average axial load. The time required for acceleration and deceleration is 0.23 sec. The maximum velocity is 0.45 m/s.

$$l_{1,4} = \frac{V_{max}*t_1}{2} * 10^3 = 104\text{mm} \quad (11)$$

$$l_{2,5} = l_s - \frac{V_{max}*t_1 + V_{max}*t_3}{2} * 10^3 = 590\text{ mm} \quad (12)$$

$$l_{3,6} = \frac{V_{max}*t_3}{2} * 10^3 = 104\text{mm} \quad (13)$$

Axial load during acceleration, deceleration, and uniform motion is to be calculated to find the average axial load.

$$F_{a1} = \mu.mg + f + m\alpha = 1906\text{N}. \quad (14)$$

$$F_{a2} = \mu.mg + f = 30\text{N}. \quad (15)$$

$$F_{a3} = \mu.mg + f - m\alpha = 1846\text{N}. \quad (16)$$

where F_{a1}= forward acceleration,F_{a2}= forward uniform motion, F_{a3} = forward deceleration. While calculating the axial load, friction in the guideway, that is the guide surface resistance(f), friction in the feed drive system ($\mu.mg$) to drive the load, have to be considered. In addition to the above, the inertia force mα has to be considered during acceleration and deceleration. Similarly, for backward acceleration (F_{a4}), backward deceleration (F_{a6}), and backward uniform motion (F_{a5}) also can be found.

$$F_{a4} = \mu.mg - f - m\alpha = -1906\text{N}. \quad (17)$$

$$F_{a5} = \mu.mg - f = -30\text{N}. \quad (18)$$

$$F_{a6} = \mu.mg - f + m\alpha = 1846\text{N}. \quad (19)$$

The average axial load during forward motion (F_{m_1}) and backward motion (F_{m_2}) are given by,

$$F_{m_1} = \sqrt[3]{\frac{F_{a_1}^3*l_1 + F_{a_2}^3*l_2 + F_{a_6}^3*l_6}{l_1+l_2+l_3+l_4+l_5+l_6}} = 951\text{N}. \quad (20)$$

$$F_{m_2} = \sqrt[3]{\frac{F_{a_3}^3*l_3 + F_{a_4}^3*l_4 + F_{a_5}^3*l_5}{l_1+l_2+l_3+l_4+l_5+l_6}} = 951\text{N}. \quad (21)$$

Since $F_{m_2} = F_{m_1}$, the average axial load is 951N. The load friction torque is given by the equation,

$$M_d = \frac{FL}{2\pi\varepsilon} = 48\text{ N-mm}. \quad (22)$$

The optimum preload is one third of the average axial load for a ball nut (20). The preload friction torque is given by the equation, where ε- efficiency of the ball screw is 0.95.

$$M_{pl} = \frac{F_{pl}L}{2\pi\varepsilon}(1-\varepsilon^2) = 43\text{N-mm}. \quad (23)$$

Total frictional torque is the sum of load torque and preload torque.

$$M = M_d + M_{pl} = 91\text{N-mm}. \quad (24)$$

Power loss due to the friction torque, generates heat. Power loss equation is given by eqn (25), where 'n' is rotational speed

P= 0.12πn M= 10W (25)

Calculation of bearing heat generation

The front bearing and rear bearing generate heat during motion of the feed drive system, the heat is generated due to the load friction (M_l) and fluid friction (M_v). The thrust load acting horizontally, drives the feed drive system. The weight of the table and weight of the component act radially downwards. Two extreme cases of bearing heat generation are taken, in case-1 ballnut is near the front bearing(B), in case-2 ball nut is near the rear bearing(A)

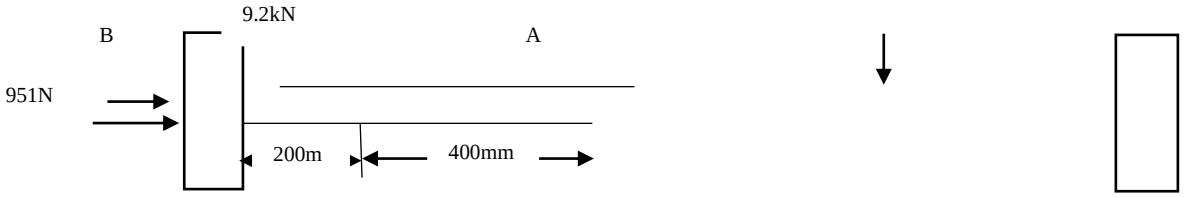

Fig.8.Load application of feed drive system in case-1

Using the equilibrium equations, the radial components of the bearing loads can be found.
Taking moments about bearing (B):

$$F_{rA} \times (600) = (9200 \times 200)$$

$F_{rA} = 3067$ N.

Taking moments about bearing (A):

$$F_{rB} \times (600) = (9200 \times 400)$$

F_{rB}= 6133N.

As angular contact bearing is used, an axial load is induced due to the applied radial load.

$F_{aB} = \frac{0.5F_{rB}}{Y}$ = 3333N. where Y is the axial load factor.

Total axial load in bearing B, is sum of axial load induced (F_{aB}) due to the radial load and thrust load.

$F_{aBtotal} = 3333 + 951 = 4284$N.

The total friction is the sum of load friction and fluid friction.

$M_l = 0.672 * 10^{-3} D_{pw}^{0.7} F_a^{1.2}$ = 179Nmm. (26)

$M_v = 3.47 * 10^{-10} D_{pw}^{3} n_i^{1.4} Z_B^{a} Q^{b}$= 10Nmm. (27)

where, pitch diameter of rolling element (D_{pw}) = 33.5mm. n_i is the rotational speed of the rolling element,z_B is the absolute viscosity of the lubricant.

$a = 24 n_i^{-0.37}$= 2.5.

$b = 4 * 10^{-9} n_i^{1.6} + 0.03$= 0.03.

a, b are constants which can be found by substituting the rotational speed. The total frictional torque(M) is given by

$$M = M_l + M_v$$

Heat generation equation is given by,

$Q = 0.105 * 10^{-6}$ Mn = 5W. (28)

Along the bearing A, the axial load acts along one direction which is the axial load induced due to the applied radial load.

$F_{aA} = \frac{0.5F_{rA}}{Y}$= 1763N.

Similar to the bearing B, the load friction torque, fluid friction torque and the total frictional torque can be calculated.

$M = M_l + M_v$=60Nmm.
The heat generated due to the friction is given by,
$Q = 0.105 * 10^{-6}$ Mn = 2W.

For case-2, the ball nut position is varied such that it is near the rear bearing, similar steps as those adopted for case-1 are followed to find out the bearing heatgeneration.
Fig.9**.** Load application of feed drive system in case-2
Heat generated in the bearings B and A for case-2 are found to be 3W and 4W respectively.

THERMOMECHANICAL ANALYSIS OF FEED DRIVE SYSTEM

The ball screw shaft is divided into number of segments, which helps in applying heat at different segments which corresponds to heat generated at different positions during the motion of the ball screw and nut.In case-1 of feed drive system, the ball screw and nut motion are in such a way that it is positioned near to the front bearing. It is assumed that the feed drive system is under free convection throughout the entire process. The heat generated in the front and rear bearings and heat generated by the ball screw and nut are applied at the corresponding locations as a boundary condition in FEA. In case -2 of feed drive system, the ball screw and nut are positioned near the rear bearing. Transient thermal coupled transient structural analysis is carried out.

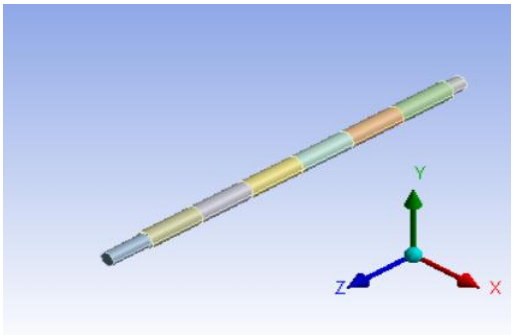

Fig.10. Ball screw shaft

The heat generated by the two bearings for the two cases are given as a heat flux in FEA analysis. Similarly, the heat generated by the ball screw and ball nut are also given as heat flux. The ball screw shaft is divided into number segments, so that heat can be applied in each portion as shown in Fig.10. Heat generated in the front and rear bearings, and ball nut are given as heat flux at their respective portions, as shown in Fig.11 and Fig.12.

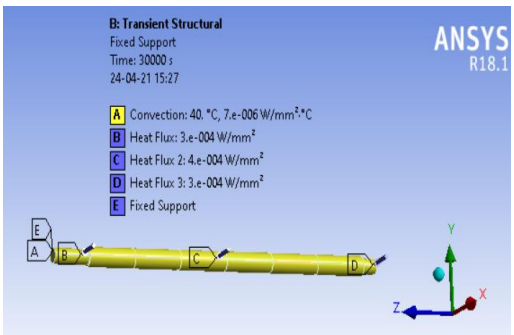

Fig.11. Case-1 boundary conditions

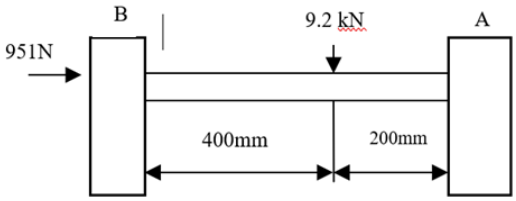

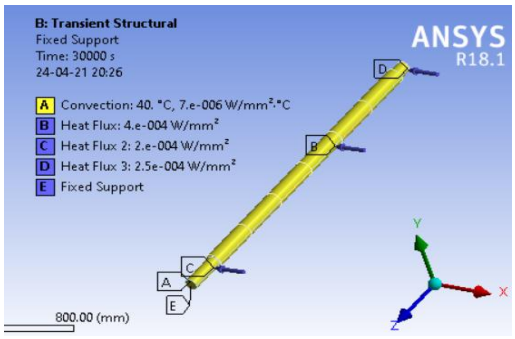

Fig.12.Case-2 boundary conditions

From Fig.13it can be observed that the temperature changes with time and attains a steady state after a certain time period. The higher temperature obtained for case-1 compared to case-2 is due to the fact that the heat generated in the front bearing is more compared to that generated in the rear bearing since back-to-back bearings (double bearings) are used for front bearing, also ball nut position is near the front bearing. The temperature from the transient thermal analysis is coupled to transient structural analysis. It is observed from Fig.14 that the deformation for case-1 is higher compared to case-2. Due to the application of axial load in two directions for case-1, more friction load torque is produced and more heat is generated, so more deformation is produced. The deformation in Fig.14 varies accordingly to the transient temperature change of the ball screw shaft, and remains constant after reaching steady state.

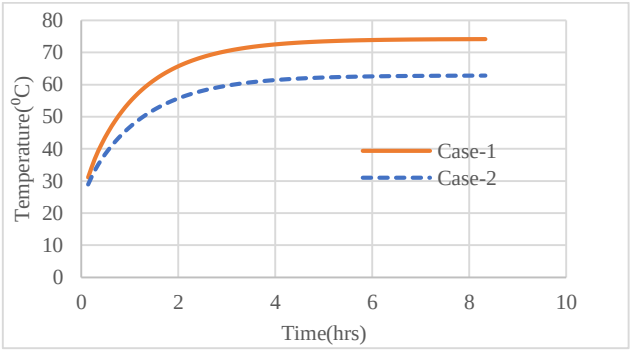

Fig.13 Transient temperature change of thefeed drive system.

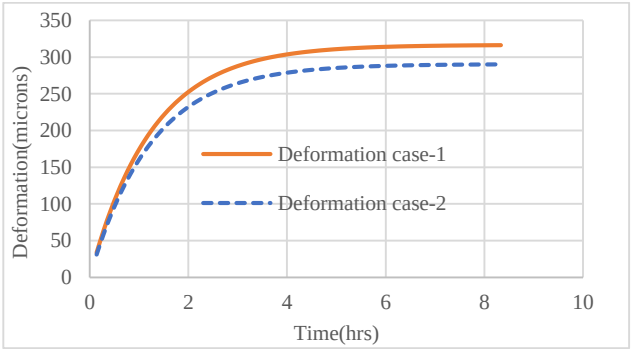

Fig.14.Transient variation ofdeformation of the feed drive system.

International Journal of Aquatic Science
ISSN: 2008-8019
Vol 12, Issue 02, 2021

MATHEMATICAL MODELLING FOR PREDICTION OF THERMAL ERRORS

Transfer function.

Transfer function is used to establish relationship between input and output of a system. Transfer function can also be defined as the ratio Laplace transform of input to the Laplace transform of output. If a system is represented by a differential equation, it is hard to deal with the differential operator. Transfer function can be used on the other hand, which is a set of algebraic or polynomial equation, it is easy to handle algebraic equations compared to differential equation. The differential equation can be converted to transfer function by taking the Laplace transform of it, and it can be solved in complex s domain(frequency), or it can be solved in time domain by taking inverse Laplace transform.

$$Y = \frac{b_m s^m + \cdots + b_1 s + b_0}{a_n s^n + \cdots + a_1 s + a_0} U \qquad (29)$$

In equation (29), Y represents the output of the system, U represents the input of the system. The polynomial term represents the transfer function. The transfer function in particular is defined by the number of poles and zeroes. The roots of numerator denote the zeroes and the root of denominator denote the number of poles. Two transfer functions are developed to predict the thermal errors of guideway and feed drive system. Temperature- deformation data from FEA are fed into the SITB and the transfer function that provides the best fit to the data can be obtained by altering the poles and zeroes of transfer function.

Determining transfer function for the guideway of the VMC base

The transfer function can be obtained from MATLAB, using system identification tool box (SITB). The SITB is a tool box used to model a system using a variety of mathematical models like transfer function, linear regression etc. By changing the number of poles and zeroes, transfer function of different order can be obtained. The transfer order which gives the best fit for our system has to be taken.The estimated transfer function for the guideway of the VMC base, for the prediction of thermal deformation along X- direction I given by equation 30. Similarly, the transfer functions for predicting the thermal deformation along Y and Z directions in the guideway of the VMC base can be determined by following similar steps.

$$T(s) = \frac{4.618e^{-06}s^3 + 6.546e^{-09}s^2 + 5.149e^{-12}s + 2.219e^{-16}}{s^4 + 0.00294\,s^3 + 3.172e^{-06}s^2 + 1.149e^{-09}s + 4.559e^{-14}} . \qquad (30)$$

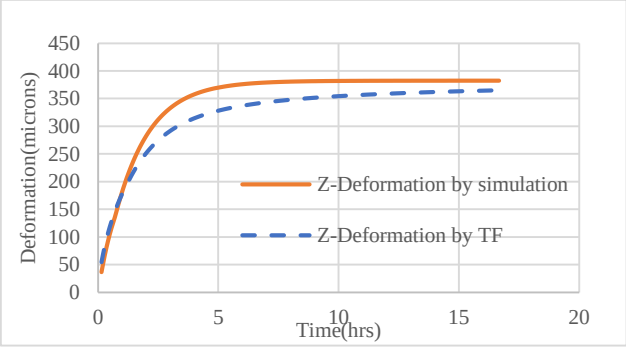

Fig.15. Deformation estimated by TF and simulation

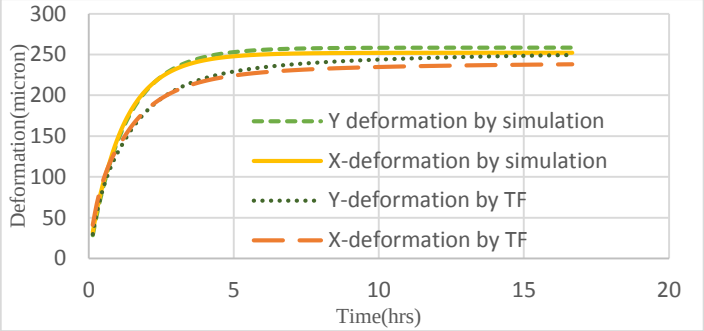

Fig.16. Deformation estimated by TF and simulation

The thermal deformation in the guideway of VMC base along the Z direction, and that along the X and Y directions are depicted in Fig.15 and Fig.16 respectively. A comparison of the deformations estimated by the transfer function method with that obtained through FEM indicates a close correlation between the two, indicating that the transfer function can be used as a reliable predictive tool. The transfer function obtained from MATLAB is also called as data driven transfer function.

Determining transfer function for feed drive system of the VMC base.

The transfer function can also be derived theoretically, apart from using SITB in MATLAB. The ball screw shaft heat generation can be approximated by using a unidimensional heat conduction equation. This approximation validates well, since the deformation along the axial direction of the shaft only contributes to the thermal error (14). The transfer function obtained from MATLAB is given by

$$T(s) = \frac{7.635e^{-06}s^2+8.909e^{-09}s+1.293e^{-12}}{s^3+0.004433s^2+2.519e^{-06}s+3.03e^{-10}} \quad . \qquad (33)$$

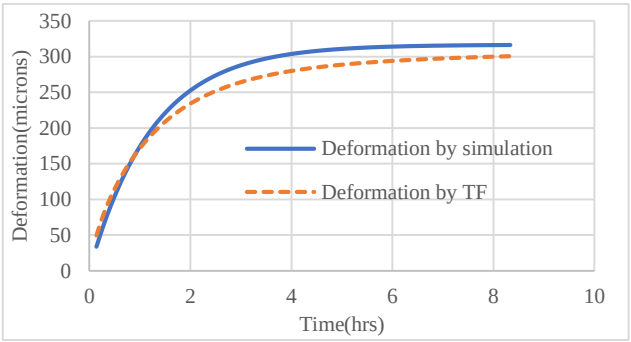

Fig.17. Case-1 deformation estimation by TF and simulation.

In Fig.17 the deformation estimated by transfer function and simulation for case-1 are compared, TF provides 85% fit. In Fig.18 the deformation estimated by TF and simulation for case-2 are compared, TF is found to provide 90% fit. The transfer function obtained provides best fit for both the cases of feed drive system

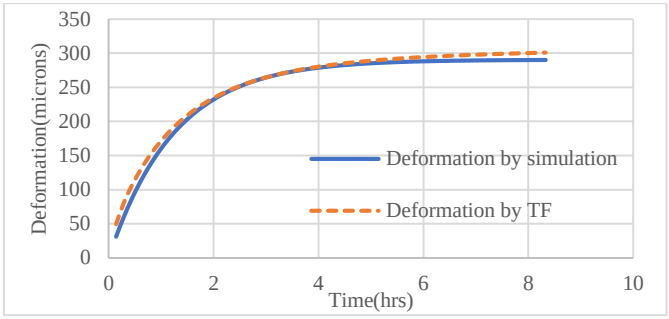

Fig.18. Case-2 deformation estimated by TF and simulation.

Data driven transfer function calculation.

The transfer function obtained from SITB in MATLAB, can be solved analytically by employing any of the two methods explained below.

Method 1: Transfer function obtained is converted to time domain by inverse Laplace transform and for the different time periods, corresponding deformation can be obtained. Temperature deformational transfer function (TDTF) is obtained from MATLAB which is shown in section VI. Similarly, thermal transfer function (TTF) can be obtained from the MATLAB, with heat source(W) as input and temperature (℃) as output.

$$\frac{Y(s)}{U(s)} = T(s)$$

T(s) is the temperature-deformational transfer function (TDTF). U(s) is the input (thermal transfer function or temperature can also be used(s) is the output(deformation).

$$Y(s) = T(s)*U(s)$$

$$Y(s) = \frac{7.635e^{-06}s^2+8.909e^{-09}s+1.293e^{-12}}{s^3+0.004433s^2+2.519e^{-06}s+3.03e^{-10}} \times TTF$$

$$TTF = \frac{0.05742s+2.729e^{-05}}{s^2+0.03244s+7.384e^{-06}} \quad . \qquad (34)$$

As the equation is in frequency domain convert it into time domain by taking inverse Laplace transform. Where Y(t), deformation in time domain can be obtained by substituting the different time periods.

Method 2: Transfer function is solved without converting it into time domain, that is, it is solved in frequency domain. It is perhaps the simplest method for solving transfer function.

$$Y(t) = \lim_{S \to 1/t} s\, U(s)\, T(s)$$

For a step input of magnitude, A. In our case, A is temperature.

$$Y(t) = \lim_{S \to 1/t} s \frac{A}{S} T(s)$$

$$Y(t) = A \lim_{S \to 1/t} T(s)$$

Here, T(s) is the Temperature deformational transfer function (TDTF). Thus, the transfer function developed can be analytically solved using the above methods and thermal error can be predicted.

2. CONCLUSION

This study investigates various heat sources, in the VMC base and thermal error(deformation) caused by them. Formulae method has been used to find out the heat generated in the guideway and feed drive system. The method is efficient since, the load variations during a cycle comprising acceleration, deceleration and uniform motion are taken into account similar to real-life situation. FEA has been carried out to find the temperature rise in the guideway and feed drive system. Transient thermal analysis is carried out to find the final temperature of the system, that is, until the system attains steady state. Thermomechanical analysis (transient thermal coupled transient structural analysis) is carried out to find thermal error(deformation) caused due to the heat generation. A mathematical model (transfer function) is developed to model the system and predict the thermal errors. Two transfer functions temperature- deformation transfer function (TDTF), and thermal transfer function (TTF) are determined. The TTF accounts for temperature rise caused by the heat sources. TDTF accounts for deformation caused by the temperature rise of the system. The transfer functions are obtained from MATLAB using SITB and are analytically solved. The results obtained from transfer function and FEA are compared. Transfer function provides a satisfactory fit to the system and prediction of thermal errors is good.

3. REFERENCES

[1] Matthias putz, Christian Opperman, Michael braunig, "Enhancement and Multi-dimensional characteristics diagram for correction of TCP displacement caused by thermal tool displacement", Procedia CIRP, Elsevier, vol 77, pp.553-556, 2018.

[2] Christian brecher, Michel klatte, Tae hun,lee,filliposTzanetos, "Metrological analysis of a mechatronic system based on novel deformation sensors for thermal issues in machine tool" , Procedia CIRP, Elsevier, vol 77, pp 517-520, 2018. .

[3] M. Putz, J.Regel, A.Wenzel, M.Braunig, "Thermal errors in milling: Comparison of displacements of the machine tool, tool and workpiece", Conference on modelling of machining operations, Elsevier, vol 82, pp. 389-394, 2019.

[4] Martin Mares, otakarhorejs, "Modelling of cutting process impact on machine tool thermal behaviour based on experimental data", Conference on modelling of machining operations, Elsevier 58, pp.152-157, 2017.

[5] Mateusz Wasiak, Arkaduiszkolka, :"Machining accuracy improvement by compensation of machine and workpiece deformation", Procedia manufacturing, Elsevier, vol 11, pp. 2187-2194, 2017.

[6] Martin Mares, OtakarHorejs, Lukas Havelik,"Thermal error compensation of a 5-axis machine tool using indigenous temperature sensors and CNC integrated Python code validated with a machined test piece", Precision engineering, vol 66, pp.21-30, 2020.

[7] O.Horejs,M.Mares,P.Kohut,P..Barta, "Compensation of machine tool thermal errors based on transfer functions", MM science journal, pp. 128, 2010.

[8] HuichengZhou,pengcheng,,Hu,Huiling, "Modelling and compensation of thermal deformation for machine tool based on the real-time data of the CNC system", Procedia manufacturing, Elsevier, vol 26, pp.1137-1146, 2018.

[9] Xaverthiem, Bernd kauschinger, Steffen Ihlenfeldt, ''Structure model-based correction of thermally induced motion errors of machine tools", Procedia manufacturing, Elsevier, vol 14, pp.128-135,2017.

[10] Sung-Hyun Jang, Gung-ho Khim, Chun-Hong Park, "Estimation of friction heat in a linear motion bearing using Box–Behnken design", International journal on advancement of manufacturing technology, Springer-Verlag London, vol 89, pp. 2021-2029, 2016.
[11] Bosch Rexroth, "Linear motion technology handbook",2017.
[12] John.FentressGardener,Bohdan Kulakowski,Jesse Lowen Shearer,"Dynamic modelling and control of Engineering systems" 2012.
[13] THK, "Linear motion handbook",2016.
[14] Ayman Abuaniza, Naeem S Mian, Simon Fletcher, Andrew P Longstaff, "Thermal error modelling of a CNC machine tool feed drive system using FEA method", IJERT, vol 5, 2018.
[15] HuichengZhou,Pengcheng, Hu,HuilingTan,"Modelling and compensation of thermal deformation for machine tool based on the real-time data of the CNC system", Procedia manufacturing, vol 26, pp.1137-1146.
[16] Kio Liu, Mingjia Sun, Yuliang Wu, "Thermal Error Modeling Method for a CNC Machine Tool Feed Drive System", Mathematical problems in engineering, vol 2015, 2015.
[17] Mahmmod Aziz Muhammed,"The effect of heat generated by friction in the ball-screw-nut system on the precision of high-speed machine", journal of techniques, vol 24, pp.112-123, 2018.
[18] Zhenjun Li, Chunyu Zhao,Fangchen Liu,Ye Chen,"Heat Source Forecast of Ball Screw Drive System Under Actual Working Conditions Based on On-Line Measurement of Temperature Sensors", MDPI sensors, vol 19, 2019.
[19] THK, "Ball screw and nut catalogue",2016.
[20] NSK, "Ball bearing catalogue",2013.